

MR Image Contrast Enhancement by Wavelet-based Contourlet Transform

Zhongliang Luo*, Yingbiao Jia

School of Information Science and Engineering

Shaoguan University

Shaoguan 512005, China

E-mails: luozl66@126.com, jiayingbiao@sgu.edu.cn

*Corresponding author

Received: January 25, 2016

Accepted: June 1, 2016

Published: June 30, 2016

Abstract: The contrast of magnetic resonance (MR) image local regions is low, edges blurred and image contains noise. To improve image contrast of local regions and solve the problem of noise enlarging, an MR image contrast enhancement algorithm by wavelet-based contourlet transform (WBCT) was put forward in this paper. Firstly, MR images were decomposed into low-pass and a series of high-pass sub-band images by WBCT, then algorithm adjustment coefficients of sub-band images were used through an enhancement operator. Finally, the contrast enhanced image was obtained by inverse WBCT. Compared with several image enhancement algorithms, the experimental results demonstrated that the ability of the proposed method in highlighting MR image's subtle features and preserving edges while suppressing noise. The contrast enhanced image had better visual effect, which is beneficial to doctor for diagnosing diseases.

Keywords: Image contrast enhancement, Wavelet-based contourlet transform, Magnetic resonance image, Nonlinear.

Introduction

Magnetic resonance (MR) imaging plays an important role in modern disease diagnosis, for it provides large amounts of complementary information. As magnetic resonance imaging technology has no ionizing radiation, is not invasive and is very safe, it is widely used in medical research and clinical diagnosis, especially for observing the changes of various brain regions within diagnosis of lesions in the human brain [13, 15]. However, due to the fact that magnetic resonance imaging equipment is affected by many factors, MR images sometimes have low contrast, these darker regions occupying a very narrow range of gray. This makes it difficult to distinguish subtle features, and even useful signal is drowned out by noise, which makes it difficult to image analysis and disease diagnosis [16]. Traditional image enhancement methods cannot deal with the problem of MR image local region enhancement and suppress noise enlarging. Therefore, a better MR image contrast enhancement method is needed.

Generally, space domain and transform domain are two commonly used image enhancement methods. Similar, the existing MR image enhancement technologies are also divided into two categories. The aim of image enhancement is to improve image visual effects, which makes image more easily analyzed by humans or computer systems. Spatial domain method, histogram equalization, image smoothing and un-sharp masking are widely used in digital image contrast enhancement. For the spatial domain method, direct operations are performed on image pixels. The formula for spatial domain method can be expressed as follows:

$$I_E(x, y) = T[I(x, y)], \quad (1)$$

where $I(x, y)$ denotes the original image (the input image), $I_E(x, y)$ is the enhanced image (the output image), and $T[\cdot]$ represents the transformation applied to the input image.

A number of enhancement methods exist in the spatial domain. References [8, 17, 18] believe that the gray scale transformation method is a relatively simple and effective way to enhance the image. These methods mainly improve the overall contrast with a simple linear or nonlinear enhancement operator without taking into account the image's local information. It cannot avoid the output image's local over-enhancing or noise amplification as the whole image contrast is enhanced. This makes it not an ideal method for MR image enhancement. Authors in [9] adopted local an adaptive histogram equalization to enhance image, however, the method has a much longer compute time.

The frequency domain method is another technique used for image enhancement. Transform domain enhancement methods involve transforming image intensity data into a specific domain by using a kind of frequency domain transform [8, 18]. Examples of frequency domain transforms include discrete Fourier transform (DFT), discrete cosine transform (DCT) and discrete wavelet transform (DWT), etc. The frequency content of the image altered with an enhancement operator. The enhanced image is obtained by inverse transformation. Magnitude and phase are components of these transformation, where magnitude represent frequency content of image and phase is useful to converting image back to spatial domain. These frequency coefficients processed by a linear or nonlinear operator, and the enhanced image is obtained by an inverse transform. The processing can be expressed as:

$$I_E(u, v) = H(u, v)I(u, v). \quad (2)$$

View from frequency domain, $G(u, v)$ represents the enhanced image, $I(u, v)$ denotes original image, $H(u, v)$ is image enhancing function and it is the key for image enhancement method.

The commonly used two dimensional wavelet transform is a separable extension of a dimensional wavelet transform, which mainly suits to a variety of objects with isotropic singularity. For the anisotropic singularity, such as digital image boundaries and linear features, wavelet transform cannot work well and is not efficient in representing contours in horizontal or vertical directions.

Recently, other new multiscale analysis methods have been developed, among which the contourlet transform [12] exhibits very high directional sensitivity and is highly anisotropic. In view of its redundancy, Eslami and Radha [6] proposed a new non-redundant image transform namely wavelet-based contourlet transform (WBCT). WBCT can achieve both radial and angular decomposition to an arbitrary extent and obeys the anisotropy scaling law. It can also easily be realized by applying DFB to wavelet coefficients of an image.

The shortcomings of the existing MR image enhancement algorithm, we propose a new image enhancement method with WBCT in this paper. It deals with low and high frequency sub-band coefficients, with linear and nonlinear processing operators respectively. It enhanced image by performing an inverse WBCT. The algorithm can enhance subtle features of local region and improve image clarity while suppressing noise enlarging, which provides a more accurate and valuable reference for clinical diagnosis.

MR image enhancement with WBCT

Contourlet transform

Over the past decade, wavelet analysis has been paid lots of attention image processing field such as image code, image de-noising and enhancement, feature extraction and edge detection [4]. For two dimensional image, wavelet is no longer the optimal basis for image, the wavelet basis function presents some limitations, due to the fact that they are not well adapted to the detection of highly anisotropic elements in image. In order to improving the representation sparsity of an image over wavelets, some new transforms have been introduced for image processing. In 2002, Do and Vetterli [4] proposed contourlet transform (CT) based on a multiscale and multidirectional filter bank which can represent natural images. With contourlet theory constantly improving, there are constant advancements in image de-noising and image fusion [4, 6].

The contourlet transform is a double iterative filter structure which deals with multiscale analysis and direction analysis respectively. It consists of two steps: sub-band decomposition and directional transform [10]. In the first step, a Laplacian pyramid (LP) is used to capture point discontinuities, then directional filter banks (DFB) are applied to each band pass channel at the second step, and point discontinuity is linked into linear structure. We can attribute the success to two properties of the contourlet transform. One is the directionality property, i.e. having basis functions at many directions while wavelet transform has only 3 directions. Another is the anisotropy property. This means that basis functions appear at various aspect ratios (depending on the scale), as opposed to at an equal aspect ratio wavelet. Fig. 1a shows contourlet transform filter structure.

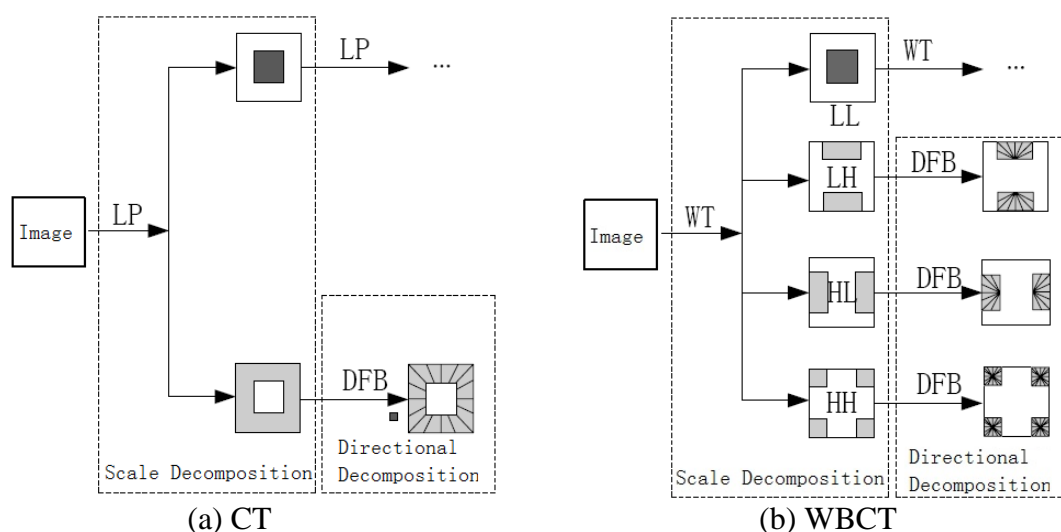


Fig. 1 The comparison of decomposition process of the first level

Wavelet-based contourlet transform

Contourlet transform can effectively present image edges, lines, curves and contours features. However, contourlet transform has a redundancy factor of 4/3. In 2004, Eslami and Radha [6] proposed a new non-redundant image transform that is WBCT. It has a similar construction to contourlet transform. It achieves both radial and angular decomposition to an arbitrary extent and obeys the anisotropy scaling law. Firstly, multiscale image decomposition is by wavelet then, each high frequency sub-band decompose with contourlet transform, adopting DFB to get further directional decomposition. As wavelet transform and DFB are non-redundant complete reconstructions, the WBCT is also a non-redundant reconstruction transformation.

The WBCT consists of two steps [7, 10]: the first step provides sub-band decomposition, using a wavelet transform rather than the Laplacian pyramid, the second step of the WBCT is a directional filter bank, which provides angular decomposition. The graph of the detail decomposition process of WBCT is shown in Fig. 1b. In the first step of WBCT, the image is decomposed into one low frequency sub-band corresponding to LL and three high-pass bands corresponding to LH, HL and HH. In the second step, DFB is performed with the same number of directions on every high frequency sub-band in a given level.

Compared with wavelet and contourlet transform, the WBCT can make full use of the unique geometrical features of an image itself, forming the most sparse image representation. Better reflecting the visual characteristics of an image, it can capture image structure features more efficiently. The MR image is decomposed by CT and WBCT, as is shown in Fig. 2. So, the WBCT is applied to MR image enhancement.

The decomposition process of WBCT can be seen from the following.

Sub-space can be obtained image $I(x, y)$ with wavelet decomposition. $W_{j,HL}, W_{j,LH}$ and $W_{j,HH}$ are image detail components in horizontal, vertical and diagonal directions of scale j respectively, and their basis functions are $\psi_{j,HL}(n), \psi_{j,LH}(n)$ and $\psi_{j,HH}(n)$. When the three sub-spaces are adopted with l_j levels of directional filtering, the k -th directional subspace will be obtained, and marked with $W_{j,HL,k}^{l_j}, W_{j,LH,k}^{l_j}$ and $W_{j,HH,k}^{l_j}$ ($0 \leq k \leq 2^{l_j}$) respectively [7]. The relation between the WBCT and wavelet space is:

$$W_{j,i} = \bigoplus_{k=0}^{2^{l_j-1}} W_{j,i,k}^{l_j}, \quad i = HL, LH, HH. \tag{3}$$

The basic functions of directional sub-bands are:

$$\eta_{j,i,k}^{l_j}(n) = \sum_{m \in \mathbb{Z}^2} g_k^{l_j}(n - S_k^{l_j} m) \psi_{j,i}(m), \tag{4}$$

where $g_k^{l_j}$ is directional filtering and $S_k^{l_j}$ is the down sampling matrix. After l_j levels of directional filtering, sub-bands can be obtained as follows:

$$c_{j,k}^{l_j}[n] = \langle I, \eta_{j,i,k}^{l_j}(n) \rangle. \tag{5}$$

The decomposition diagram of CT and WBCT are given in Fig. 2a and 2b which combine 3 layers of wavelet decomposition and 3 levels of DFB for the MR image. The direction number is 8, with each level from the finest level to coarse level. It obtains 48 sub-bands.

Elimination of artifacts

Due to the DFB step of WBCT, down-sampling is involved. It is a shift variant, which will lead to the image producing a certain ‘winding’ phenomenon. Therefore, image may appear to have pseudo Gibbs distortion, interference fringes, visual artifacts or blurring of the feature on image edges and important details. To compensate for lacking of the translation invariance

property of WBCT, cycle spinning is adopted to improve image enhancement performance. Cycle spinning method [3, 9, 11] is expressed as:

$$\hat{S} = \frac{1}{N_1 N_2} \sum_{i=1, j=1}^{N_1, N_2} S_{-i, -j} (T^{-1} f [T (S_{i, j} (I(x, y)))]), \quad (6)$$

where $S_{i, j}$ and f respectively represent circulated shift and its enhancement operator, N_1, N_2 are the maximum number of shifts in the row and column directions, $i_1, j_1, -i_1, -j_1$ represent the number of shifts in the row and column directions, T and T^{-1} express the transform operator and its inverse transform.

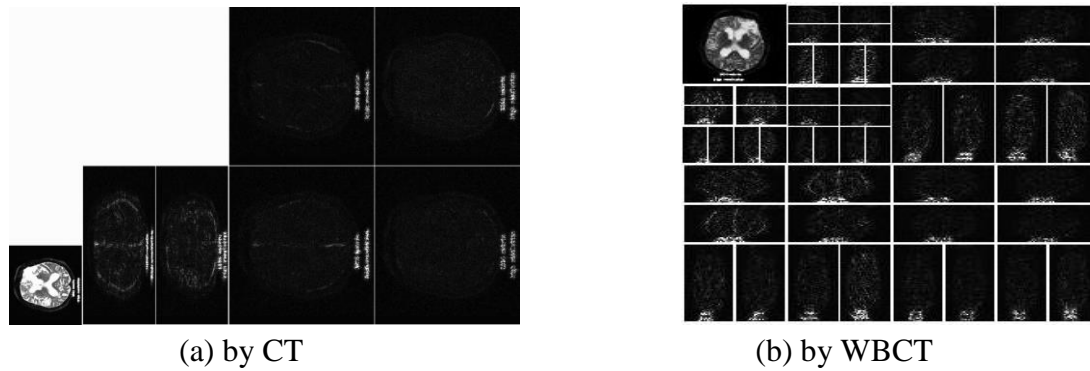


Fig. 2 Comparison of image decomposition

MR image enhancement by WBCT

After image is decomposed with WBCT, it obtains a low-frequency sub-band image and many high-frequency sub-band images, i.e. $I_L(x, y)$:

$$I(x, y) = I_L(x, y) + \sum_{l=1}^N \omega_k^l(x, y), \quad (7)$$

where $\omega_k^l(x, y)$ represents high-frequency sub-band images decomposed by contourlet at different scales and directions

$$\omega_k^l(x, y) = I_k^l(x, y) - I_{k-1}^l(x, y). \quad (8)$$

To deal with image decomposition coefficient, sub-band coefficients are first normalized, so that $I_L(x, y) \in [-1, 1]$ and $\omega_k^l(x, y) \in [-1, 1]$.

Using WBCT to decompose the MR image, it generates approximate and detail coefficients. Since approximate and detail coefficients represent low-pass and band-pass sub-images respectively, they are thus treated in different ways during the enhancement processing.

The commonly used image nonlinear enhancement operator

The classic generalized adaptive gain (GAG) nonlinear processing method was used to enhance features in digital mammography, which was proposed in [9]:

$$E_{GAG}(v) = \begin{cases} 0 & |v| < T_1 \\ \text{sign}(v)T_2 + \bar{a}(\text{sigm}(c(u-b)) - \text{sigm}(-c(u+b))) & T_2 \leq |v| \leq T_3, \\ v & \text{otherwise} \end{cases} \quad (9)$$

where $E_{GAG}(v)$ is the normalized multiscale transform coefficients, b is a parameter to control enhancement range, c is gain factor, $u = \text{sigm}(v)(|v| - T_2)/(T_3 - T_2)$ and $\bar{a} = a(T_3 - T_2)$.

However, this operator involves several parameters, such as b , c , T_1 , T_2 , T_3 . In practice, these parameters need constant adjustment to achieve better enhancement, which is bound to affect its practical applications.

GAG output curve is shown in Fig. 3.

Another commonly used nonlinear enhancement operator was proposed by Starck et al. [14]. It can be seen as follows:

$$y_c(x, \sigma) = \begin{cases} 1 & \text{if } x < c_1 \cdot \sigma \\ \frac{x - c_1 \sigma}{c_1 \sigma} \left(\frac{m}{c_1 \sigma} \right)^p + \frac{2c_1 \sigma - x}{c_1 \sigma} & \text{if } x < 2c_1 \sigma \\ \left(\frac{m}{x} \right)^p & \text{if } 2c_1 \sigma \leq x < m \\ \left(\frac{m}{x} \right)^s & \text{if } 2x \geq m \end{cases}, \quad (10)$$

where factor p determines the degree of nonlinear transform; x are curvelet coefficients; m is threshold; s decides to dynamic compress range; c_1 is the regularization parameter; and σ represents noise standard. Its enhancement curve can be seen in Fig. 4.

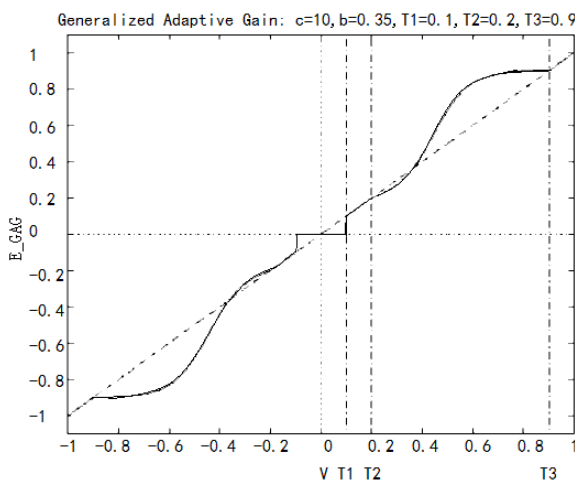


Fig. 3 The GAG enhancement curve

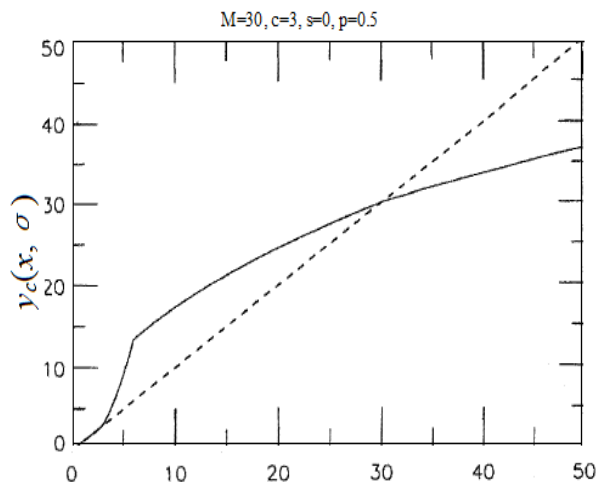


Fig. 4 The curvelet enhancement curve

Low-pass sub-band coefficient adjustment

The low-pass sub-band image reflects the basic overview of original image, it contains a large amount of image information. In order to effectively improve overall contrast of the original image, we use linear enhancement operator to adjust coefficients, then they are expanded.

$$En_I_L(x, y) = \frac{I_L(x, y) - \min[I_L(x, y)]}{\max[I_L(x, y)] - \min[I_L(x, y)]}, \quad (11)$$

where $I_L(x, y)$ is normalized coefficients of low-pass sub-band, $\min[I_L(x, y)]$ is the minimum and $\max[I_L(x, y)]$ represents the maximum value of each sub-band coefficient.

High-pass sub-band coefficients nonlinear adjustment

The low-pass sub-band image reflects the basic overview of original image, it contains a large amount of image information. The band-pass directional sub-band contains edge detail information and noise. According to coefficient amplitude, the coefficients fall into three types: strong edge, weak edge and noise. For the strong edge, its coefficient of each direction is larger. For the weak edge, only a certain direction is larger, but coefficients of noise are small in any direction [5]. The purpose of image enhancement is to enlarge weak edges and restrain noise. Therefore, the high frequency sub-band coefficients of WBCT are classified with a threshold, and image is enhanced by nonlinear adjustment to the high-pass sub-band image:

$$I_i(x, y) = \begin{cases} E_s, & \bar{\omega}_k^l \geq Th_k^l \\ E_w, & 0.5 \cdot Th_k^l \leq \bar{\omega}_k^l \leq Th_k^l, \\ n & \bar{\omega}_k^l < 0.5 \cdot Th_k^l \end{cases} \quad (12)$$

where E_s and E_w represents the strong edge and weak edge, n denotes noise, Th_k^l is the sub-band threshold of scale l and direction k , $\bar{\omega}_k^l$ represents the average of the sub-band coefficient of $\omega_k^l(x, y)$, $m_1 \times n_1$ is the size of high sub-band image:

$$Th_k^l = \frac{1}{2} \sqrt{\frac{1}{m_1 \times n_1} \sum_{x=1}^{m_1} \sum_{y=1}^{n_1} [\omega_k^l(x, y) - \bar{\omega}_k^l]^2}. \quad (13)$$

Therefore, a simple, practical, low complexity image enhancement algorithm is proposed in this paper, which uses a nonlinear mapping function to modify band-pass sub-band coefficients. The nonlinear enhancement operator is fast, monotonous, has adjustable parameters and it meets image enhancement requirements. According to decomposition coefficients amplitude and image correlation, the operator increases certain range of transform coefficients and enhance subtle edge hidden in background, ensuring certain scope coefficient get amplified. In this paper, the nonlinear enhancement operator is as follows:

$$I_o(x_{i,j}) = \begin{cases} x_{i,j}, & x_{i,j} \in E_s \\ x_{i,j} \cdot \text{sign}(x_{i,j}) \cdot \tanh(b \cdot u) \cdot (1 + c \cdot \exp(-u \cdot u)), & x_{i,j} \in E_w, \\ 0, & x_{i,j} \in n \end{cases} \quad (14)$$

where $u = 2 \cdot \frac{x_{i,j} \cdot [\max(x_{i,j}) - \min(x_{i,j})]}{t \cdot \max(x_{i,j})}$, in which u is a coefficient amplitude in transform

domain. In this formula, $t \cdot \max(x_{i,j})$ is a threshold which shows that the coefficients larger than this threshold will be linearly amplified. The parameters b and c are essential to image enhancement. To determine the expanded range, b is a parameter to control the critical point of enhancement curve and ensure many sub-band coefficients are enhanced, c controls the shape of the nonlinear function curve. Its enhancement curve can be seen in Fig. 5.

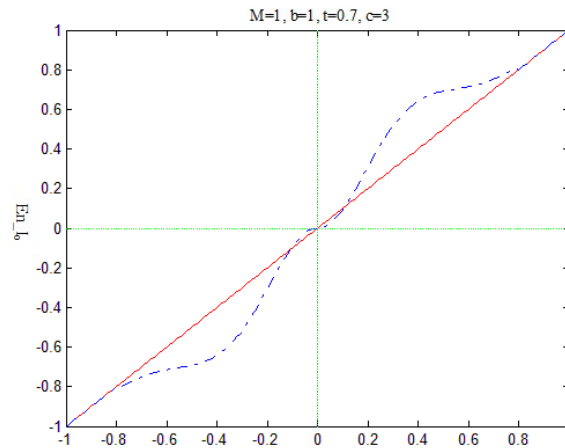


Fig. 5 The enhancement operator of the proposed algorithm

As can be seen from Eq. (14), the nonlinear function is smoother than the piecewise linear function, and the contrast enhanced image will be relatively smooth. So, the strong edge of image is retained, and the weak edge is enhanced with noise effectively suppressed.

Image enhancement algorithm overview

The proposed MR image enhancement algorithm can be described by the following seven major steps:

- (1) Using cycle spinning to shift MR image, the maximum number of cycles translations will be k ($n = 2^k$).
- (2) Carrying out WBCT for the cyclic translated image, and obtaining coefficients of different scales in different directions.
- (3) Using two image enhancement operator to adjust low-pass and high-pass sub-band coefficients respectively.
- (4) Performing inverse WBCT on modified coefficients.
- (5) Implementing inverse shift to reconstruct the image \hat{S} , and averaging over all results to get the enhanced image.
- (6) Adjusting global contrast of MR image by gamma correction.
- (7) Using peak signal to noise ratio, information entropy, contrast improvement index and edge preservation index to evaluate the quality of the enhanced image.

Experimental results and analysis

Evaluation index

The image enhancement result can be evaluated from both a qualitative and a quantitative criteria perspective. Qualitative analysis relies mainly on visual image, its evaluation is

somewhat subjective. However there is the question of how to use the quantitative method to evaluate result of enhancement as there is no uniform evaluation criteria at present. It is generally considered that a good image needs to contain more information such as appropriate brightness, contrast and clarity. Peak signal to noise ratio can measure the denoising performance of the algorithm with the higher the peak signal to noise ratio, the better the enhancement performance. Information entropy represents the image information's ability to carry details. Contrast improvement index represents the overall image detail enhancement, where a larger contrast denotes more information may be seen. Edge preservation index reflects the enhanced image with respect to the edges information of original image, the greater the value of edge preservation index, the better indication of image quality. In this paper, peak signal to noise ratio, information entropy, contrast improvement index and edge preservation index are used to evaluate the effect of MR image contrast enhancement.

The peak signal to noise ratio (*PSNR*), information entropy (*H*), contrast improvement index (*CII*) and edge preservation index (*EPI*) are defined as [1, 2, 17-19]:

$$PSNR = 10 \lg \left(\frac{255^2}{\frac{1}{M \cdot N} \sum_{x=1}^M \sum_{y=1}^N [I_E(x, y) - I(x, y)]^2} \right), \quad (15)$$

where $I(x, y)$ is the original image pixel intensity value for the pixel location (x, y) , $I_E(x, y)$ is the enhanced image pixel intensity value for the pixel location (x, y) , $M \cdot N$ is the size of original image.

$$H = - \sum_{k=0}^m \frac{A_k}{M \cdot N} \log_2 \frac{A_k}{M \cdot N}, \quad (16)$$

where A_k ($k=0, 1, \dots, m$) is the number of pixels with k representing gray in the whole image, and m representing the maximum gray scale.

$$CII = \sqrt{\frac{\sum_{x=1}^M \sum_{y=1}^N [I(x, y) - \bar{I}]^2}{M \cdot N}}, \quad (17)$$

where \bar{I} represents the average of the whole image $I(x, y)$ gray value.

$$EPI = \frac{\sum (|I_E(x, y) - I_E(x+1, y)| + |I_E(x, y) - I_E(x, y+1)|)}{\sum (|I(x, y) - I(x+1, y)| + |I(x, y) - I(x, y+1)|)}. \quad (18)$$

Test results

To verify the performance of image contrast enhancement algorithm, two MR images were tested with several algorithms. The algorithm was simulated in Matlab 2012a, using a running environment of an Intel 3.2 GHz, 4GB of RAM for PC. The MR image was decomposed by WBCT with two layers of wavelet decomposition and three DFB combinations of method; wavelet transforms with "Haar" wavelet basis; DFB decomposition adopt McClellan transform using "9-7" filter; and obtained 48 sub-bands. To verify the effect of the algorithm,

histogram equalization (HE), un-sharp masking enhancement, image enhancement with wavelet transform and contourlet transform were applied to MR image in the experiment respectively. Fig. 6 and Fig. 7 are the two original images and their enhanced images using several comparison methods. Table 1 shows test data in Fig. 6 and Fig. 7.

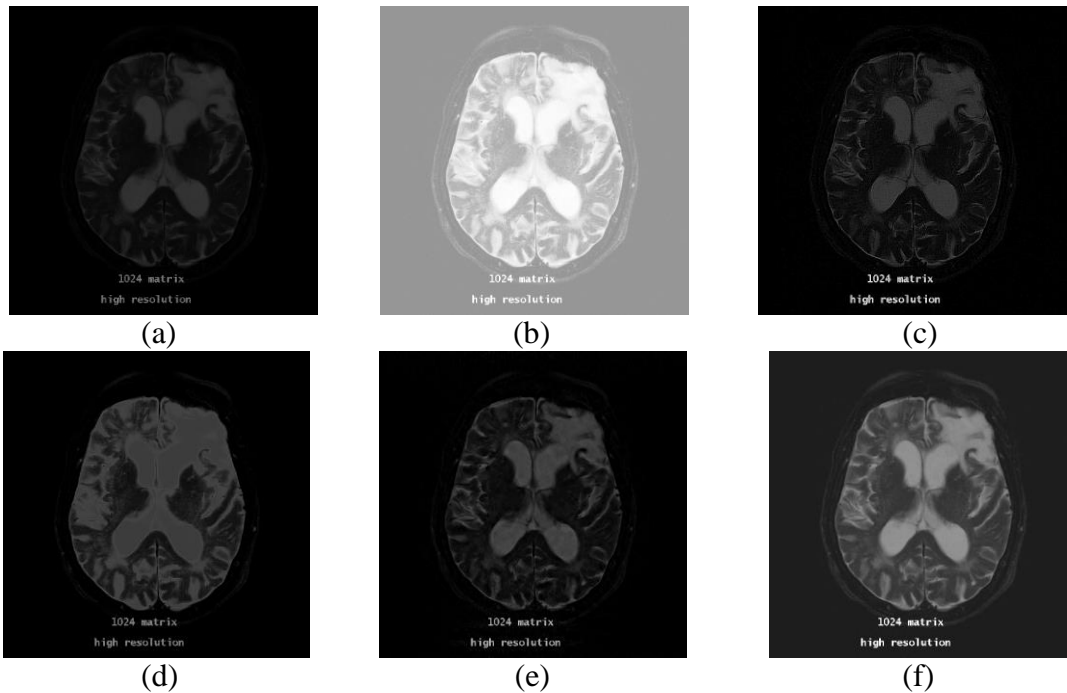


Fig. 6 MR1 and its enhanced image with enhancement method:
(a) original; (b) histogram equalization; (c) un-sharp masking;
(d) wavelet; (e) CT; (f) the proposed algorithm.

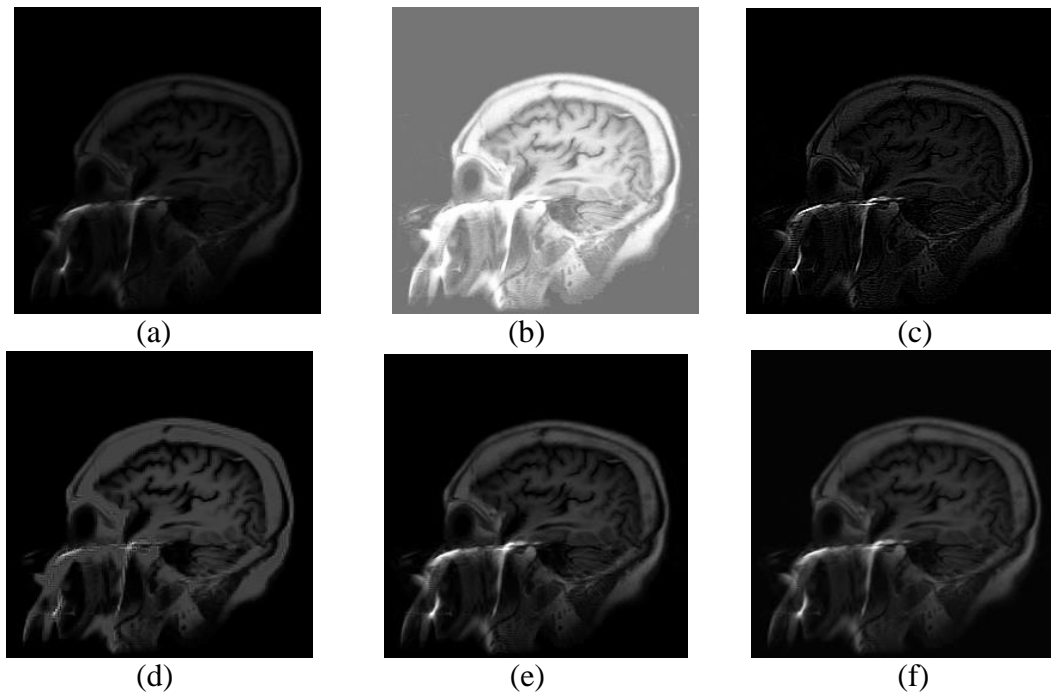


Fig. 7 MR2 and its enhanced image with enhancement method:
(a) original; (b) histogram equalization; (c) un-sharp masking;
(d) wavelet; (e) CT; (f) the proposed algorithm.

Table 1. Objective evaluation index comparison for the enhanced image

Images		<i>PSNR</i>	<i>H</i>	<i>CII</i>	<i>EPI</i>
Fig. 6	(b)	51.99409	2.45023	55.38076	1.28580
	(c)	65.08630	3.15670	28.86839	1.42232
	(d)	73.43446	3.31111	42.93297	1.63732
	(e)	75.94843	4.03815	29.53803	1.73231
	(f)	77.04497	4.42140	45.49689	1.83124
Fig. 7	(b)	52.78159	3.64199	40.26128	1.36640
	(c)	79.27337	3.65110	12.06314	1.14435
	(d)	71.39276	4.15858	19.73805	1.87792
	(e)	71.19509	4.50465	21.01909	1.94017
	(f)	72.87570	4.62987	22.64459	1.98279

Results analysis

Before image enhancement, the human brain MR image contrast was insufficient, the whole background was dark and detailed information hidden in higher and lower gray areas was difficult to distinguish. From Fig. 6 and Fig. 7, image contrast had improved and subtle features could be seen, but the image was partially bright and it seemed to be rather stiff. The histogram equalization algorithm had a simple average image gray value, its image contrast was enhanced while noise was obviously amplified, original detail information in light or dark areas was concealed. Un-sharp masking enhancement can improve a visual effect, but image contrast is not obvious. For the wavelet image enhancement method, the enhancement image exhibited Gibb's phenomenon with loss of some detail texture information and image was blurred.

The proposed algorithm was the best in many regards including: visual effect; it had no obvious artifacts; the image was clearer than before, which can show image edge details better; and noise was effectively suppressed while image detail was enhanced, as is shown (f) in Fig. 7 and Fig. 8. Table 1 shows data for the information entropy, *PSNR*, *CII* and *EPI*. Among them, the histogram equalization method was the lowest, while the proposed method was the best, thus it can provide more relevant and accurate diagnosis information. The histogram equalization method enlarged noise so its information entropy decreased.

All enhancement algorithms, the contrast, clarity and *PNSR* were improved to some extent, but the entropy and peak signal to noise ratio of the proposed algorithm was the highest among the five enhancement methods.

Fig. 8 is the histogram of Fig. 6. Among them, Fig. 8a is the histogram of the original image, whose gray was mainly concentrated under 0.23. Fig. 8b concentrated on gray between 0.58~1, so the image was bright, however, the enhanced image with the proposed method in Fig. 8f had well distributed gray between 0~0.53 and 0.92~0.96. The image's dynamic range stretching and visual effect had been improved and some darker details were seen more clearly. In short, whether from a subject or object aspect, to evaluate image enhancement effect, the comparative experimental results indicate that the proposed MR image contrast enhancement method produced a better outcome, which improved the image's visual effects proving to be of greater assistance for diagnosis.

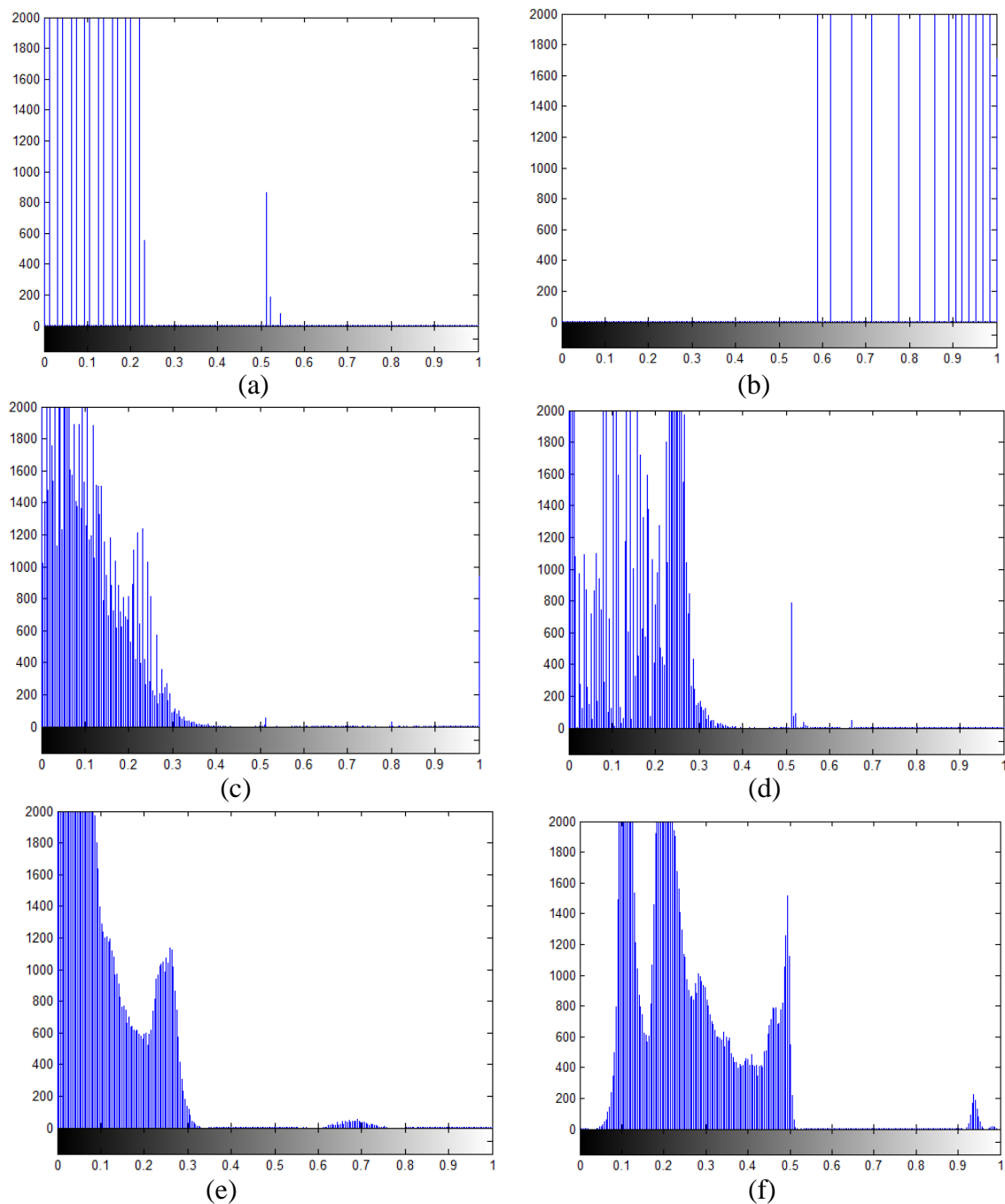


Fig. 8 Histogram comparison of images:
(a) Fig. 6a, (b) Fig. 6b, (c) Fig. 6c, (d) Fig. 6d, (e) Fig. 6e, (f) Fig. 6f.

Conclusion

We proposed an efficient and simple method for MR image contrast enhancement based on WBCT. Using a multi-directional and multi-scale of WBCT to express image features, image contrast was enhanced with two nonlinear enhancement operators by processing each sub-band coefficients. Cycle spinning was introduced for WBCT to eliminate image distortion due to the WBCT lacking in translation invariance. The proposed method focused on improving the visibility of image based on quality metrics like *PSNR*, *H*, *CII*, *EPI*. The method was tested on MR images and compared with four enhancement methods. Some exciting results were obtained which prove that the proposed method can effectively enhance subtle features while suppressing noise and preserving the main structures. The difficult problem of noise

amplification and contrast enhancement was solved, which provides greater assistance for diagnosing diseases from MR images. For further research, the running time of the enhancement algorithm in real time still needs improvement.

Acknowledgements

This work was supported by Guangdong Natural Science Foundation (Grants No. 2016A030307044, S2012040007376, 2014A030313700) and Science and Technology Planning Project of Shaoguan (Grant No. 2013CX/K70).

References

1. Amutha S., D. R. Ramesh Babu, R. Shankar, H. Kumar (2013). MRI Denoising and Enhancement Based on Optimized Single-stage Principle Component Analysis, *International Journal of Advances in Engineering and Technology*, 5(2), 224-230.
2. Cai J., T.-X. Wu, K. Zhou, W. Li (2015). Recognition of Osteoporosis Based on Texture Analysis and a Support Vector Machine, *International Journal Bioautomation*, 19(1), 107-118.
3. Coifman R. R, D. L. Donoho (1995). Translation Invariant Denoising, *Springer Lecture Notes in Statistics: Wavelets and Statistics*, 103, 125-150.
4. Do M. N., M. Vetterli (2005). The Contourlet Transform: An Efficient Directional Multiresolution Image Representation, *IEEE Transactions on Image Processing*, 14(12), 2091-2106.
5. Dong L., Y. Bing, Y. Mey (2008). Image Enhancement Based on the Nonsubsampled Contourlet Transform and Adaptive Threshold, *Acta Electronica Sinica*, 36(3), 527-530 (in Chinese).
6. Eslami R., H. Radha (2004). Wavelet-based Contourlet Transform and Its Application to Image Coding, *Proceedings of the International Conference on Image Processing*, 3189-3192.
7. Gao X. B., W. Lu, X. L. Li, D. Tao (2008). Wavelet-based Contourlet in Quality Evaluation of Digital Images, *Neurocomputing*, 72(3), 378-385.
8. Gayathri S., N. Mohanapriya, B. Kalaavathi (2013). Survey on Contrast Enhancement Techniques, *International Journal of Advanced Research in Computer and Communication Engineering*, 2(11), 4176-4180.
9. Jin Y. P., L. M. Fayad, A. F. Laine (2001). Contrast Enhancement by Multiscale Adaptive Histogram Equalization, *Proc SPIE*, 4478, 206-213.
10. Liu G. (2012). The Translation Invariant Wavelet-based Contourlet Transform for Image Denoising, *Journal of Multimedia*, 7(3), 254-261.
11. Liu K., G. Lei, J. S. Chen (2011). Contourlet Transform for Image Fusion Using Cycle Spinning, *Journal of Systems Engineering and Electronics*, 22(2), 353-357 (in Chinese).
12. Nezhdarya E., M. B. Shamsollahi (2006). Image Contrast Enhancement by Contourlet Transform, *Proceeding of 48th International Conference on Multimedia Signal Processing and Communications*, 81-84.
13. Nithiya R., S. Anadalatchoumy, R. Vithiya, A. Sundaravadivelan (2013). An Efficient Image Segmentation of Contrast Enhanced MR Images of Brain Tumor, *International Journal of Scientific and Engineering Research*, 4(4), 747-754.
14. Starck J. L., F. Murtagh, E. J. Candes, D. L. Donoho (2003). Gray and Color Image Contrast Enhancement by the Curvelet Transform, *IEEE Transactions on Image Processing*, 12(6), 706-717.
15. Tateyama T., Z. Nakao, X. Han, Y.-W. Chen (2009). Contrast Enhancement of MR Brain Images by Canonical Correlations Based Kernel Independent Component Analysis, *International Journal of Innovative Computing Information and Control*, 5(7), 1857-1866.

16. Tian X., J. Yin, Y. Sun (2008). A Simple Enhancement Algorithm for MR Head Images, Lecture Notes in Computer Science, Medical Imaging and Informatics, 4987, 57-62.
17. Wang J., G. Q. Wang, M. Li, W. Du, W. Yu (2015). Hand Vein Images Enhancement Based on Local Gray-level Information Histogram, International Journal Bioautomation, 19(2), 245-258.
18. Yadav A., B. Singh, S. Singh (2011). Comparative Analysis of Different Enhancement Method on Digital Mammograms. International Conference on Computer and Communication Technology, 159-163.
19. Zong X. L., F. K. Andrew (1998). Speckle Reduction and Contrast Enhancement of Echocardiograms via Multiscale Nonlinear Processing, IEEE Transactions on Medicine Image, 17(4), 532-540.

Assoc. Prof. Zhongliang Luo, Ph.D.

E-mail: luozl66@126.com



Zhongliang Luo received his Ph.D. degree from South China University of Technology in 2010. Now he is an Associate Professor at Shaoguan University. His major research interests include digital image processing, biometrics, and medical signal processing.

Yingbiao Jia, Ph.D.

E-mail: jjayingbiao@sgu.edu.cn



Yingbiao Jia received his Ph.D. degree from Northwestern Polytechnical University in 2014. He is currently a lecturer at Shaoguan University. His main research interests are digital image processing and compressive sensing.